Determination of Relative Stabilities of Metal-Peptide Bonds in the Gas Phase

Monika Cziferszky,*[a] Dianna Truong,[b] Christian G. Hartinger,[b] and Ronald Gust[a]

Abstract: Understanding binding site preferences in biological systems as well as affinities to binding partners is a crucial aspect in metallodrug development. We here present a mass spectrometry-based method to compare relative stabilities of metal-peptide adducts in the gas phase. Angiotensin 1 and substance P were used as model peptides. Incubation with isostructural *N*-heterocyclic carbene (NHC) complexes of Ru^{II}, Os^{II}, Rh^{III}, and Ir^{III} led to the formation of various adducts, which were subsequently studied by energy-resolved fragmentation experiments. The gas-phase stability of the metal-peptide bonds depended on the metal and the binding partner. Of the four complexes used, the Os^{II} derivative bound strongest to Met, while Ru^{II} formed the most stable coordination bond with His. Rh^{III} was identified as the weakest peptide binder and Ir^{III} formed peptide adducts with intermediate stability. Probing these intrinsic gas-phase properties can help in the interpretation of biological activities and the design of site-specific protein binding metal complexes.

Introduction

Metal complexes provide extensive chemical space to develop novel drugs, including geometries and functional groups that are inaccessible by purely organic compounds. A range of fast-developing analytical techniques are being used to study metal-based drugs and their speciation, targets, and metabolites, which enables the community to understand the modes-of-action of some approved metallodrugs and an ever increasing number of new promising metal complexes.[1] Cisplatin for example, a widely used chemotherapeutic agent, exerts its anticancer activity mainly through binding to two adjacent guanine residues in DNA, which ultimately leads to cell death.[2] Auranofin, used in the treatment of rheumatoid arthritis, inhibits the enzyme thioredoxin reductase through coordination to selenocysteine in its active site.[3] Exploring unknown mechanisms of action is pivotal in the design and synthesis of the next generation of metal-based drug candidates, and endeavors in metallodrug development are shifting towards more rational design.[4]

Biological environments are rich in potential ligands for metal ions. The molecular interactions of a metal complex and any biomolecule usually involve the formation of one or more dative bonds. Lewis bases such as thiol groups and amines in amino acids or N7 in purine nucleobases can coordinate to various metal centers. Although HSAB (hard soft acid base) theory provides some guidance, general rules for binding site preferences in biomolecules are difficult to establish, since other factors including surface charge of the biomolecule and lipophilicity of the metal complex play a role.[5] Also, non-covalent (mainly electrostatic) interactions may be involved in the initial binding of the metal complex prior to coordinative bond formation.[6] Numerous studies examining the metalation of peptides,[7] proteins[8] and oligonucleotides[9] have been published in the last two decades. Pioneering work on establishing binding preferences of metallodrugs were performed by Casini et al.[10] using both Pt^{II} and Ru^{II} complexes in a competitive assay with three proteins. Artner et al.[11] investigated the binding selectivity of two different Ru^{II} complexes using capillary zone electrophoresis-mass spectrometry and found preferential binding to guanine in nucleotides for one of the compounds and a preference for protein binding (on Met) for the other one. A similar effect has been observed by switching from an *S,N*- to an *O,N*-coordination motif in organo-ruthenium compounds, which renders a complex from a protein binder to a DNA-targeting agent.[12] In a series of competitive experiments Meier et al.[13] investigated the binding selectivity of Au^{III} complexes towards relevant biomolecules including selenocysteine and could relate their molecular reactivity to the respective biological effects.

The stability of biomolecule–metal bonds is critical for the modes-of-action of metal-based agents. Non-specific binding to highly abundant proteins or small molecules such as glutathione may have a role in transport or inactivation of the drug, depending on the reversibility of binding.[14] The direct meas-

[a] *Dr. M. Cziferszky, Prof. R. Gust*
Department of Chemistry and Pharmacy, Institute of Pharmacy
University of Innsbruck
Innrain 80–82, A-6020 Innsbruck (Austria)
E-mail: monika.cziferszky@uibk.ac.at

[b] *D. Truong, Prof. C. G. Hartinger*
School of Chemical Sciences, University of Auckland
Private Bag 92019, Auckland 1142 (New Zealand)

Supporting information for this article is available on the WWW under https://doi.org/10.1002/chem.202102385

urement of metal-protein affinities, i.e., their dissociation constants, in solution is challenging and complicated.[15] Qualitative studies on the stability of model peptide–metal complex adducts employing competition experiments revealed that glutathione is able to cleave Ru moieties from the model protein ubiquitin.[14b,16]

Mass spectrometry (MS) has been used at different levels of metallodrug mode-of-action studies on account of its high sensitivity and ability to analyze complex samples.[17] Both top-down and bottom-up methods have extensively been used to investigate the molecular interactions of metallodrugs with peptides, proteins, and oligonucleotides.[18] These approaches provide information about the nature and stoichiometry of metal ion–biomolecule adducts as well as binding site preferences. MS-based metalloproteomics methods have recently shown first successes in identifying protein targets, which is considered one of the main challenges in the field.[1d,19]

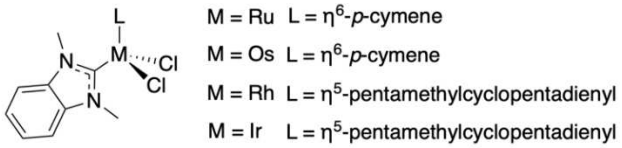

Figure 1. General structure of the anticancer metal-NHC complexes.

In an approach to expand the MS toolbox with a complementary method, we used energy-resolved mass spectrometry (ER-MS) to gain insight into the stability of metal complex–biomolecule adducts in the gas phase. The absence of solvent effects and other influences in the high vacuum of the mass spectrometer provide an ideal basis to measure intrinsic properties of the ions of interest. The relative bond stabilities measured in the gas phase correlate to properties in the condensed phase.[20]

Results and Discussion

To delineate the differences in peptide interaction endowed by the metal centers of bioorganometallic compounds, we aimed to investigate complexes with structures as similar as possible. We chose the isostructural metal–NHC complexes, i.e., [Ru(NHC)(cym)Cl_2], [Os(NHC)(cym)Cl_2], [Rh(NHC)(Cp*)Cl_2], and [Ir(NHC)(Cp*)Cl_2] (Figure 1; cym = η^6-*p*-cymene, Cp* = η^5-pentamethylcyclopentadienyl, NHC = 1,3-dimethylbenzimidazol-2-ylidene), some of which show anticancer and thioredoxin reductase inhibitory activity,[21] and investigated their molecular interactions with the model peptides angiotensin 1 (AT) and substance P (SubP) and in particular the stability of the newly formed metal-peptide bond (Figures 2–4).

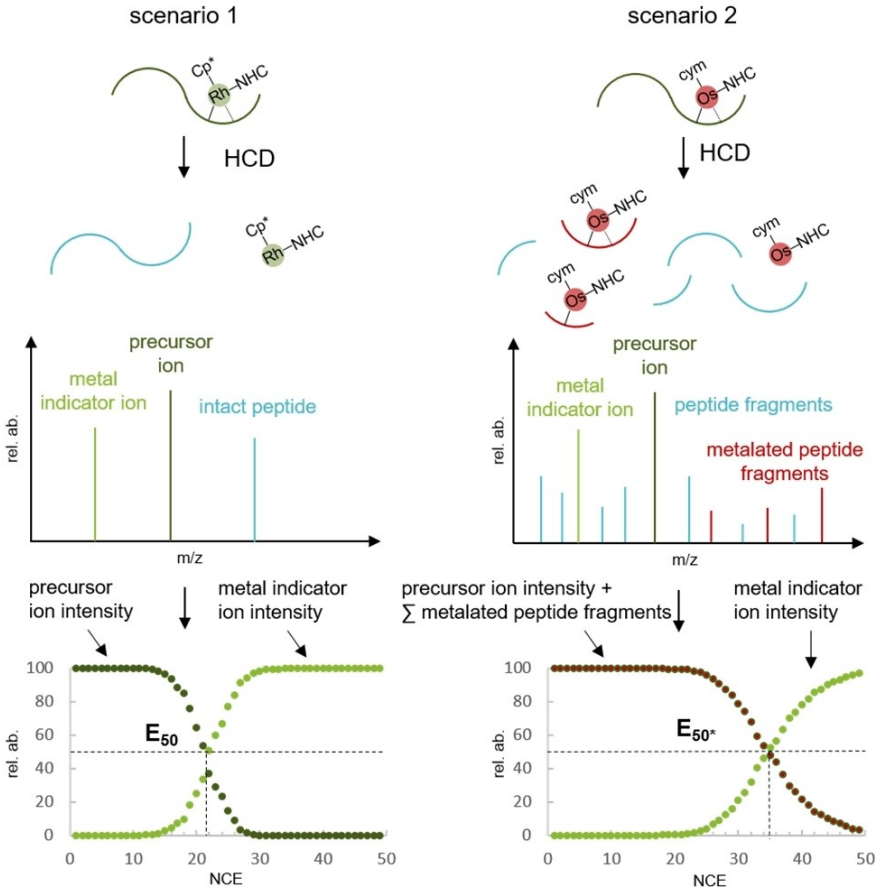

Figure 2. General concept describing the two different fragmentation scenarios and the determination of E_{50}/E_{50*} values.

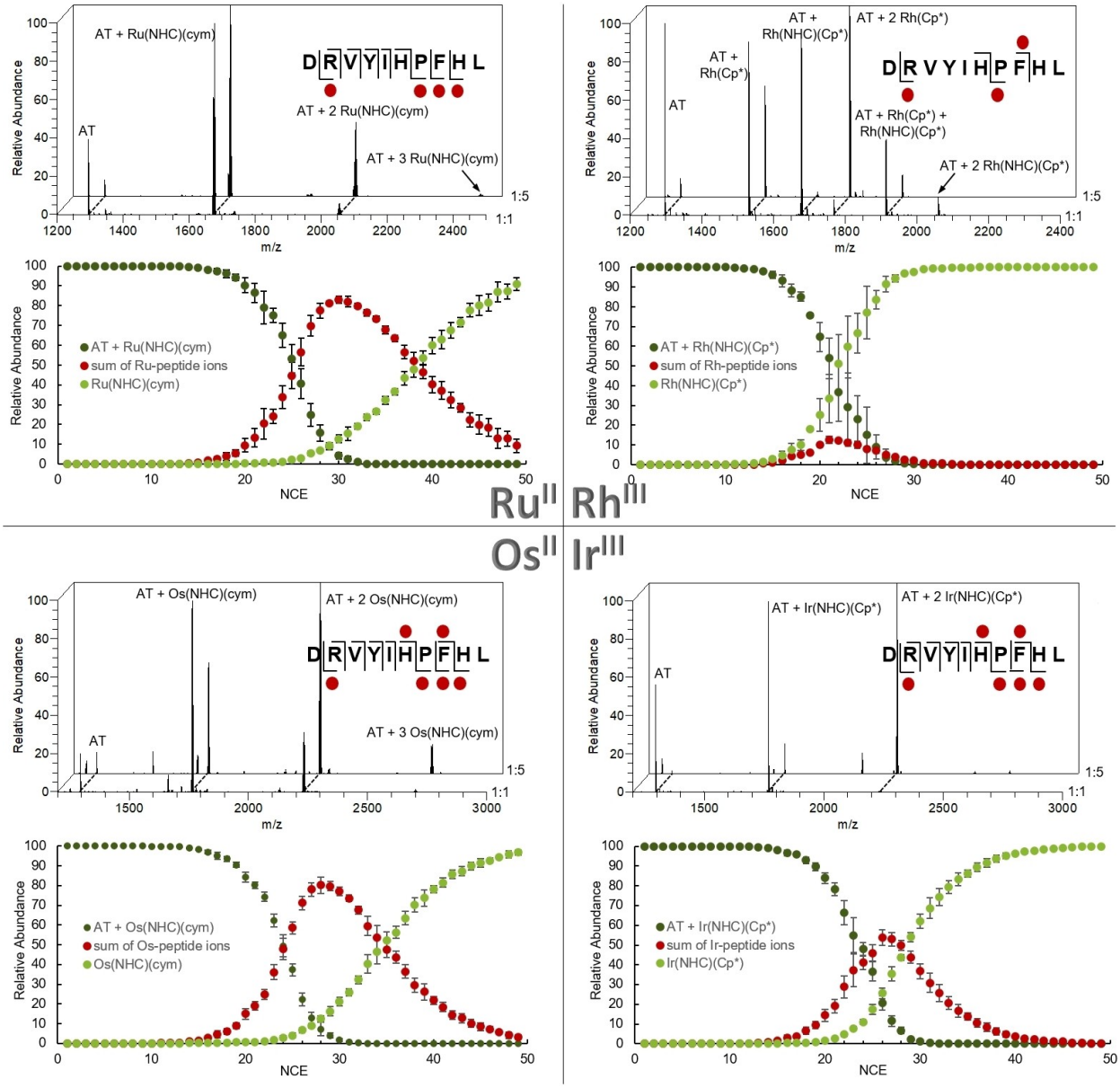

Figure 3. Deconvoluted mass spectra of AT after incubation with the metal complexes for 24 h (top) and the corresponding breakdown curves of the 1:1 adducts [AT + M(NHC)(cym/Cp*)] in charge state +3. Ion intensities were calculated as mean values plus/minus standard deviation from two independent experiments at three different time points.

The model peptides (100 μM in Milli-Q water) were incubated at equimolar ratios and five-fold excess with the metal complexes for 7 days and samples were taken at intervals. High resolution mass spectra of diluted samples (1:100 with 50/50 ACN/H_2O containing 0.1% formic acid) were recorded on an Orbitrap Elite ESI-MS (Thermo Scientific) in positive ion mode. In all cases, the formation of 1:1 adducts [peptide + M(NHC)(cym/Cp*)] was observed in high abundance within 24 h (see Figures 3 and S1), with the ions mainly detected as triply charged species $[peptide + M(NHC)(cym/Cp^*) + H]^{3+}$. During formation of the Rh adduct with AT, the NHC ligand was found to be released easily and a [AT + Rh(Cp*)] adduct was detected at higher abundance than [AT + Rh(NHC)(Cp*)], a behavior that has also been noticed when hen egg white lysozyme crystals were soaked with the Rh^{III} complex.[22] The chlorido ligands appear to be very labile under the conditions used, as in neither case chlorido complexes were observed. The remaining coordination site on the metal centers may be occupied through bidentate binding of the peptide or a loosely bound solvent molecule.

In general, more adduct formation was observed for AT than for SubP. AT contains two His residues which are known to have affinity for metal ions like Ru^{II},[23] Os^{II},[24] Rh^{I},[25] Rh^{III},[26] Ir,[III][27] and Pt^{II}.[28] AT adducts with two M(NHC)(cym/Cp*) groups attached were found in high abundance when the metal complexes were used in five-fold excess. In the sequence of

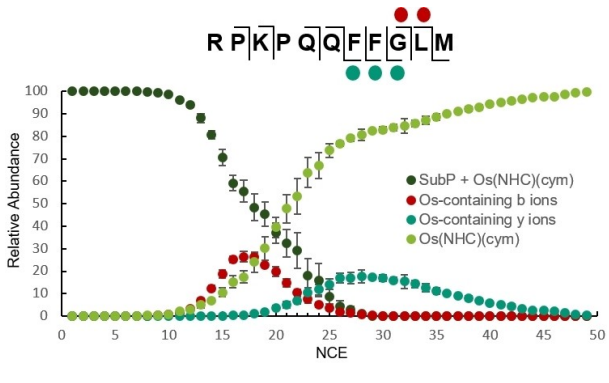

Figure 4. Fragmentation map and breakdown curve of [SubP + Os-(NHC)(cym)] adducts. The stepwise appearance of Os-containing b and y ions indicates two binding sites with differing stability.

SubP, the *C*-terminal Met amide, and *N*-terminal Arg and Lys residues provide potential binding sites for metals. The lower abundance of SubP adducts compared to AT adducts suggests that the metal complexes investigated have lower affinity for those binding partners as compared to His, or that binding sites are less accessible. Even when an excess of the metal complexes was used, a two-fold metalation of SubP was only observed with [Os(NHC)(cym)Cl_2].

MS^2 experiments allow for in-depth characterization of any gaseous ion of interest by a variety of ion dissociation techniques.[29] We used higher-energy collisional dissociation (HCD) to analyze the 1:1 M(NHC)(cym/Cp*) adducts of AT and SubP. In HCD experiments, the isolated ions of interest are accelerated into a multipole collision cell, where they collide with a neutral collision gas. The energy applied for acceleration translates to normalized collision energy (NCE). With increasing size of a molecule, more energy can be dissipated in the form of vibrational energy before dissociation occurs. However, higher charge states of the same sized ion fragment at lower collision energies due to charge repulsion effects. The concept of NCE as implemented in modern MS compensates for these mass and charge dependencies. Therefore, if significantly different NCE values are observed for the dissociation of metal-peptide adducts, one can interpret these as different gas phase stabilities of the corresponding ions. This technique is generally referred to as energy-resolved mass spectrometry (ER-MS)[30] and, among others, has been used to determine relative ligand-binding strengths in metal complexes with low molecular-weight ligands.[20a,31]

Only triply-charged adduct ions were used for the energy-resolved fragmentation experiments and all other parameters, including sample preparation and instrument parameters, were kept constant. Ions of interest were isolated with an isolation width of 7 m/z and subjected to HCD with stepwise increase of fragmentation energy from 0–50 units of NCE using the "scan activation parameters" function of the Tune software provided by Thermo Scientific. When the metalated peptides were subjected to increasing amounts of NCE, one of two breakdown scenarios was observed (Figure 2); 1) The metal-peptide bond was cleaved first, leading to a metal indicator ion [M(NHC)(cym/Cp*)–H]$^+$ and an intact peptide ion [peptide + 2H]$^{2+}$. 2) The first bonds to break were peptide backbone and/or sidechain bonds resulting in a number of metalated and non-metalated peptide fragments, but no signal for the intact peptide. With increasing NCE the metal indicator fragment was eventually released from these metalated peptide fragments.

Plotting the relative abundances of the precursor ions and the metal indicator ions against the NCE provides information about the gas phase stability of the metal-peptide bond. The amount of NCE required for 50% loss of the precursor ion intensity is generally denoted as E_{50} (Figure 2). For scenario 2, the E_{50} values are equal for the unmodified peptide and metalated peptides, because the decline in precursor ion intensity is exclusively caused by peptide bond cleavages. Hence, metalated peptide intensities were added to the precursor ion intensity and plotted in relation to the metal indicator ion intensity against NCE. Hereby, we obtained values that describe the amount of energy required to break the metal-peptide bond, regardless of other inter-peptide bonds that may break first, which we termed E_{50*}.

The appearance of metalated peptide fragments allows for binding site identification. Figure 3 shows the mass spectra, fragmentation maps, and breakdown curves of AT-metal adducts. With an excess of metal complex in the incubation mixture, both His residues of AT were metalated. At equimolar ratios, His9 was preferred over His6 as binding site, as deduced from the high abundance of metalated y2-y4 ions for Ru^{II}, Os^{II}, and Ir^{III} (Table S1). This preference may be related to the proximity to Phe, which is able to form secondary π-stacking interactions, as has been shown for Ru^{II}(arene) complexes by MS[23] and in the solid state.[32] The less-abundant metalated fragments b6 and b8 for Os^{II}, Rh^{III}, and Ir^{III} indicate secondary binding to His6 (see Figure 3 and Table S1). Ru^{II} containing b6 and b8 fragments were only present in the 1:5 experiments. Notably, all metalated peptide fragments contained both the cym/Cp* and the NHC ligand. Peptide fragments bearing a metal with no ancillary ligands were not observed in this study, but are quite common for other metal complexes, for example Pt^{II}.[33]

Energy-resolved fragmentation experiments were performed for samples collected at different time points, i.e., after 1 h, 24 h, and 7 days of incubation. Fragmentation patterns and corresponding ion intensities did not change over time, hence mean values were calculated from all experiments. In the used instrumental setup, we found that peptide bonds typically break at a NCE between 20 and 30.

The breakdown curves of AT adducts with Ru-, Os-, and Ir(NHC)(cym/Cp*) (in dark green in Figure 3) follow the same path, showing a decline to 50% relative abundance at approximately 25 units of NCE, as found for unmodified AT, i.e. the E_{50} values for these ions are equal. Only [AT + Rh(NHC)(Cp*)] fragmented at slightly lower NCE (ca. 21), and led mainly to [AT + 2H]$^{2+}$ and the corresponding [Rh(NHC)(Cp*) − H]$^+$ ions, with only Rh^{III}-containing peptide fragments of low abundance. Based on our definition of the two different breakdown scenarios, the Rh^{III} adduct of AT follows scenario 1, while the adducts with Ru^{II}, Os^{II}, and Ir^{III} dissociate according to scenario 2.

The latter showed highly abundant metalated peptide fragments, mainly y2-y4, that further cleaved the metal indicator ions at NCE values above 30. As shown in Figure 3, the abundance of metalated peptide fragments and the NCE required to cleave the metal moiety are distinctly different for Ru^{II}, Os^{II}, and Ir^{III}. To describe the relative stability of the metal-peptide bond in scenario 2, we introduced the E_{50*} values (Figure 2). Here, the sum of the precursor ion intensities plus those of all the metalated peptide fragments were plotted in relation to the metal indicator ion against the NCE. This energy value describes the amount of collision energy that is required to break the metal-peptide bond regardless of other inter-peptide bonds that may break first. The E_{50*} values that were obtained for AT adducts are listed in Table 1. According to these results, Ru(NHC)(cym) forms the strongest coordination bond with the imidazole moiety in His9, followed by Os-(NHC)(cym) and Ir(NHC)(Cp*) with 5 NCE units difference in their corresponding E_{50*} values. The Rh^{III}–His bond is cleaved with the least amount of energy. Because of its higher oxidation state and small ionic radius, Rh^{III} is considered the hardest and Os^{II} the softest Lewis acid of the four metals used in this study.

The order of metal ion-peptide bond stability found here is likely caused by a combination of kinetic and thermodynamic factors. Ru^{II} seems to be the best match for the imidazole nitrogen ligand, while Os^{II} is bound more weakly due to its slightly greater softness. Rh^{III} and Ir^{III} have a higher charge density, which increases their level of hardness, that appears to be less suited for the imidazole nitrogen ligand. Ir^{III} complexes are kinetically more inert than Rh^{III}, which explains why Rh^{III} was cleaved off the peptide easiest. Also, the NHC ligand dissociated from Rh^{III} to a large extent in the AT adducts.

SubP formed 1:1 adducts with the four metal complexes to a lesser extent than AT (Figure S1). Unreacted SubP remained the most abundant species after 24 h incubation with a five-fold excess of Ru^{II}, Rh^{III}, and Ir^{III} complex. Only the Os^{II} adduct was observed in high abundance. Energy-resolved HCD experiments showed dissociation of the SubP metal adducts according to scenario 1 for the Ru^{II}, Rh^{III}, and Ir^{III} complexes with similar fragmentation energies (Table 1). Notably, redox reactions were observed for Rh and Ir. Upon fragmentation of $[SubP + Rh(NHC)(Cp^*) + H]^{3+}$, two Rh species were detected, i.e., $[Rh(NHC)(Cp^*) + H]^{+}$ with m/z 385.11 and $[Rh(NHC)(Cp^*) - H]^{+}$ with m/z 383.10 corresponding to Rh^{I} and Rh^{III} species, respectively. Similarly, using a five-fold excess of Ir^{III} complex caused the formation of the SubP adducts $[SubP + Ir(NHC)(Cp^*) + H]^{3+}$ and $[SubP + Ir(NHC)(Cp^*) + 3H]^{3+}$ with the Ir centers in oxidation states +I and +III, respectively (Table S2). Data analysis of the HCD experiments was hampered by overlapping isotopic patterns for the Ir^{I} and Ir^{III} adducts and the corresponding metal indicator fragments, but it was clearly visible that Ir^{I} cleaved at low NCE (ca. 7), while Ir^{III} required more energy to dissociate (Figure S1). A b10 fragment was also visible for the Ir^{III} adduct, although at low abundance.

Table 1. Relative stabilities of [peptide + M(NHC)(cym/Cp*)] adducts.

Adduct	Scenario	Primary binding site	E_{50}/E_{50*} [NCE]
AT + Ru(NHC)(cym)	2	His9	38.4 ± 0.6
AT + Os(NHC)(cym)	2	His9	33.6 ± 0.8
AT + Rh(NHC)(Cp*)	1	His6/9	22.4 ± 1.2
AT + Ir(NHC)(Cp*)	2	His9	28.6 ± 0.3
SubP + Ru(NHC)(cym)	1	Met11	13.1 ± 1.2
SubP + Os(NHC)(cym)	2	Met11	21.4 ± 1.0
SubP + Rh(NHC)(Cp*)	1	Met11	10.5 ± 1.2
SubP + Ir(NHC)(Cp*)	1	Met11	14.0 ± 1.2

The Os^{II} compound interacted significantly different with SubP compared to the other three metal complexes. Fragmentation of the [SubP + Os(NHC)(cym)] adduct followed scenario 2 and led to the detection of peptide fragments bearing Os moieties (Figure 4). Interestingly, b9-b10 appeared at significantly lower NCE values than y3-y5, which indicates binding to two different sites on SubP with dissimilar stabilities. Detection of b fragments points towards binding via an *N*-terminal nitrogen-containing ligand, i.e., Arg1 or Lys3, and y3-y5 suggests coordination through the sulfur in Met11.

The course of the breakdown curves looked similar for all four metal complexes with the parent ion decay being not sigmoidal, which most likely indicates two binding sites with different stabilities also for the Ru^{II}, Rh^{III}, and Ir^{III} complexes. Due to the lack of metalated peptide fragments detected, we can only assume Met11 to be the primary binding site for Ru^{II}, Rh^{III}, and Ir^{III} metal complexes. Met residues have also been reported by O'Connor et al. as preferential but weak binding sites for an Ir(Cp*) complex on calmodulin.[34] A basic nitrogen atom in Lys, Arg or the *N*-terminal amino group seems most likely as the secondary binding site. E_{50} and E_{50*} values, as listed in Table 1, describe the overall stability of metal SubP adducts, but cannot differentiate between the two binding sites. The relative order of stability found here can again be explained under consideration of HSAB theory. Os^{II} being the softest metal used within this study exhibits strongest binding to the soft sulfur nucleophile in Met11, while Rh^{III} is considered harder and consequently forms the weakest coordination bond with Met. Ru^{II} and Ir^{III} show intermediate softness and their adducts with SubP are found to be slightly more stable than with Rh^{III}.

Conclusion

Metallodrugs usually form dative bonds with biological nucleophiles with varied stability. The selectivity and reversibility of these interactions dictate the biological response upon metal complex treatment ranging from the desired activity to drug inactivation or side effects. Measuring dissociation constants of metal ion-biomolecule conjugates in solution is challenging and time-consuming. Consequently, a MS-based method providing relative stability data in a quick and simple manner can help to interpret biological activities in the complex setting of solutions and physiological environments.

In our model system consisting of two peptides with His and Met residues, known for high metal ion affinity, and four isostructural metal-NHC complexes, we observed the highest stability for the Ru^{II}-His bond and weakest interactions for Rh^{III} with Met, while the binding preference followed HSAB theory rules.

The ER-MS method presented here adds new analytical capability to gain information about molecular interactions between metal-based drugs and biomolecules and paves the way toward a more comprehensive perspective on metal–biomolecule interactions and binding preferences. Importantly, this concept opens up possibilities to elucidate more general trends on the preferential interaction of metal ions with proteinaceous targets and the respective relative gas phase stabilities, which can then be correlated to biological activities and properties in more general terms. For example, the method could be used to elucidate the molecular mechanism of thioredoxin reductase inhibition by $[Rh(NHC)(Cp^*)Cl_2]$ and support the development of more effective inhibitors.

Acknowledgements

We thank the Universities of Innsbruck and Auckland and the Kate Edger Educational Charitable Trust for financial support.

Conflict of Interest

The authors declare no conflict of interest.

Keywords: energy-resolved mass spectrometry · metallodrugs · NHC complexes · peptide metalation · relative stability

[1] a) E. J. Anthony, E. M. Bolitho, H. E. Bridgewater, O. W. L. Carter, J. M. Donnelly, C. Imberti, E. C. Lant, F. Lermyte, R. J. Needham, M. Palau, et al., *Chem. Sci.* **2020**, *11*, 12888–12917; b) S. M. Meier-Menches, C. Gerner, W. Berger, C. G. Hartinger, B. K. Keppler, *Chem. Soc. Rev.* **2018**, *47*, 909–928; c) B. Englinger, C. Pirker, P. Heffeter, A. Terenzi, C. R. Kowol, B. K. Keppler, W. Berger, *Chem. Rev.* **2019**, *119*, 1519–1624; d) T. R. Steel, C. G. Hartinger, *Metallomics* **2020**, *12*, 1627–1636.
[2] J. N. Burstyn, W. J. Heiger-Bernays, S. M. Cohen, S. J. Lippard, *Nucleic Acids Res.* **2000**, *28*, 4237–4243.
[3] S. J. Berners-Price, A. Filipovska, *Metallomics* **2011**, *3*, 863–873.
[4] C. N. Morrison, K. E. Prosser, R. W. Stokes, A. Cordes, N. Metzler-Nolte, S. M. Cohen, *Chem. Sci.* **2020**, *11*, 1216–1225.
[5] M. Hanif, C. G. Hartinger, in *Advances in Inorganic Chemistry, Volume 75 Medicinal Chemistry* (Eds: P. J. Sadler, R. van Eldik), Elsevier Inc., **2020**, p. 339–359.
[6] A. Casini, G. Mastrobuoni, M. Terenghi, C. Gabbiani, E. Monzani, G. Moneti, L. Casella, L. Messori, *J. Biol. Inorg. Chem.* **2007**, *12*, 1107–1117.
[7] a) C. A. Wootton, C. Sanchez-Cano, A. F. Lopez-Clavijo, E. Shaili, M. P. Barrow, P. J. Sadler, P. B. O'Connor, *Chem. Sci.* **2018**, *9*, 2733–2739; b) M. N. Wenzel, S. M. Meier-Menches, T. L. Williams, E. Rämisch, G. Barone, A. Casini, *Chem. Commun. (Camb.)* **2018**, *54*, 611–614; c) A. Pratesi, C. Gabbiani, E. Michelucci, M. Ginanneschi, A. M. Papini, R. Rubbiani, I. Ott, L. Messori, *J. Inorg. Biochem.* **2014**, *136*, 161–169.
[8] a) D. Gibson, C. E. Costello, *Eur. Mass Spectrom.* **1999**, *5*, 501–510; b) I. Khalaila, C. S. Allardyce, C. S. Verma, P. J. Dyson, *ChemBioChem* **2005**, *6*, 1788–1795; c) E. Moreno-Gordaliza, B. Cañas, M. A. Palacios, M. M. Gómez-Gómez, *Anal. Chem.* **2009**, *81*, 3507–3516; d) J. Li, L. Yue, Y. Liu, X. Yin, Q. Yin, Y. Pan, L. Yang, *Amino Acids* **2016**, *48*, 1033–1043; e) L. Massai, C. Zoppi, D. Cirri, A. Pratesi, L. Messori, *Front. Chem.* **2020**, *8*, 581648; f) N. C. Korkola, E. Hudson, M. J. Stillman, *Metallomics* **2021**, *13*, mfab023.
[9] a) A. Dorcier, P. J. Dyson, C. Gossens, U. Rothlisberger, R. Scopelliti, I. Tavernelli, *Organometallics* **2005**, *24*, 2114–2123; b) A. E. Egger, C. G. Hartinger, H. Ben Hamidane, Y. O. Tsybin, B. K. Keppler, P. J. Dyson, *Inorg. Chem.* **2008**, *47*, 10626–10633; c) M. Groessl, Y. O. Tsybin, C. G. Hartinger, B. K. Keppler, P. J. Dyson, *J. Biol. Inorg. Chem.* **2010**, *15*, 677–688; d) C. A. Wootton, C. Sanchez-Cano, H.-K. Liu, M. P. Barrow, P. J. Sadler, P. B. O'Connor, *Dalton Trans.* **2015**, *44*, 3624–3632.
[10] A. Casini, C. Gabbiani, E. Michelucci, G. Pieraccini, G. Moneti, P. J. Dyson, L. Messori, *J. Biol. Inorg. Chem.* **2009**, *14*, 761–770.
[11] C. Artner, H. U. Holtkamp, W. Kandioller, C. G. Hartinger, S. M. Meier-Menches, B. K. Keppler, *Chem. Commun. (Camb.)* **2017**, *53*, 8002–8005.
[12] S. M. Meier, M. Hanif, Z. Adhireksan, V. Pichler, M. Novak, E. Jirkovsky, M. A. Jakupec, V. B. Arion, C. A. Davey, B. K. Keppler, et al., *Chem. Sci.* **2013**, *4*, 1837–1846.
[13] S. M. Meier, C. Gerner, B. K. Keppler, M. A. Cinellu, A. Casini, *Inorg. Chem.* **2016**, *55*, 4248–4259.
[14] a) A. R. Timerbaev, C. G. Hartinger, S. S. Aleksenko, B. K. Keppler, *Chem. Rev.* **2006**, *106*, 2224–2248; b) C. G. Hartinger, A. Casini, C. Duhot, Y. O. Tsybin, L. Messori, P. J. Dyson, *J. Inorg. Biochem.* **2008**, *102*, 2136–2141.
[15] Z. Xiao, A. G. Wedd, *Nat. Prod. Rep.* **2010**, *27*, 768–789.
[16] S. M. Meier, M. Hanif, W. Kandioller, B. K. Keppler, C. G. Hartinger, *J. Inorg. Biochem.* **2012**, *108*, 91–95.
[17] C. G. Hartinger, M. Groessl, S. M. Meier, A. Casini, P. J. Dyson, *Chem. Soc. Rev.* **2013**, *42*, 6186–6199.
[18] M. Wenzel, A. Casini, *Coord. Chem. Rev.* **2017**, *352*, 432–460.
[19] S. M. Meier, D. Kreutz, L. Winter, M. H. M. Klose, K. Cseh, T. Weiss, A. Bileck, B. Alte, J. C. Mader, S. Jana, et al., *Angew. Chem. Int. Ed. Engl.* **2017**, *56*, 8267–8271; *Angew. Chem.* **2017**, *129*, 8379–8383.
[20] a) M. Satterfield, J. S. Brodbelt, *Inorg. Chem.* **2001**, *40*, 5393–5400; b) C. A. Schalley, *Mass Spectrom. Rev.* **2001**, *20*, 253–309.
[21] a) D. Truong, M. P. Sullivan, K. K. H. Tong, T. R. Steel, A. Prause, J. H. Lovett, J. W. Andersen, S. M. F. Jamieson, H. H. Harris, I. Ott, et al., *Inorg. Chem.* **2020**, *59*, 3281–3289; b) N. Y. S. Lam, D. Truong, H. Burmeister, M. V. Babak, H. U. Holtkamp, S. Movassaghi, D. M. Ayine-Tora, A. Zafar, M. Kubanik, L. Oehninger, et al., *Inorg. Chem.* **2018**, *57*, 14427–14434.
[22] M. P. Sullivan, M. Cziferszky, I. Tolbatov, D. Truong, D. Mercadante, N. Re, R. Gust, D. C. Goldstone, C. G. Hartinger, *Angew. Chem. Int. Ed.* **2021**, *60*, 19928–19932; *Angew. Chem.* **2021**, *131*, 20081–20085.
[23] R. H. Wills, A. Habtemariam, A. F. Lopez-Clavijo, M. P. Barrow, P. J. Sadler, P. B. O'Connor, *J. Am. Soc. Mass Spectrom.* **2014**, *25*, 662–672.
[24] C. K. C. Chiu, Y. P. Y. Lam, C. A. Wootton, M. P. Barrow, P. J. Sadler, P. B. O'Connor, *J. Am. Soc. Mass Spectrom.* **2020**, *31*, 594–601.
[25] I. M. Daubit, M. P. Sullivan, M. John, D. C. Goldstone, C. G. Hartinger, N. Metzler-Nolte, *Inorg. Chem.* **2020**, *59*, 17191–17199.
[26] C. A. Wootton, A. J. Millett, A. F. Lopez-Clavijo, C. K. C. Chiu, M. P. Barrow, G. J. Clarkson, P. J. Sadler, P. B. O'Connor, *Analyst* **2019**, *144*, 1575–1581.
[27] M. Caterino, A. A. Petruk, A. Vergara, G. Ferraro, D. Marasco, F. Doctorovich, D. A. Estrin, A. Merlino, *Dalton Trans.* **2016**, *45*, 12206–12214.
[28] M. Cziferszky, R. Gust, *J. Biol. Inorg. Chem.* **2020**, *25*, 285–293.
[29] L. A. Macias, I. C. Santos, J. S. Brodbelt, *Anal. Chem.* **2020**, *92*, 227–251.
[30] a) C. M. Crittenden, L. D. Akin, L. J. Morrison, M. S. Trent, J. S. Brodbelt, *J. Am. Soc. Mass Spectrom.* **2017**, *28*, 1118–1126; b) M. Romanczyk, Y. Zhang, M. Easton, W. Li, J. Viidanoja, H. Kenttämaa, *J. Am. Soc. Mass Spectrom.* **2020**, *31*, 58–65.
[31] a) E. Altuntaş, A. Winter, A. Baumgaertel, R. M. Paulus, C. Ulbricht, A. C. Crecelius, N. Risch, U. S. Schubert, *J. Mass Spectrom.* **2011**, *47*, 34–40; b) A. Briš, J. Jašík, I. Turel, J. Roithová, *Dalton Trans.* **2019**, *48*, 2626–2634.
[32] M. P. Sullivan, M. Groessl, S. M. Meier, R. L. Kingston, D. C. Goldstone, C. G. Hartinger, *Chem. Commun. (Camb.)* **2017**, *53*, 4246–4249.
[33] M. Cziferszky, R. Gust, *J. Inorg. Biochem.* **2018**, *189*, 53–57.
[34] Y. Qi, Z. Liu, H. Li, P. J. Sadler, P. B. O'Connor, *Rapid Commun. Mass Spectrom.* **2013**, *27*, 2028–2032.

Manuscript received: July 2, 2021
Accepted manuscript online: September 23, 2021
Version of record online: October 21, 2021

